2009

Porosity and Permeability in Ternary Sediment Mixtures

Jason Dennis Esselburn
Wright State University

POROSITY AND PERMEABILITY IN TERNARY SEDIMENT MIXTURES

A thesis submitted in partial fulfillment
of the requirements for the degree of
Master of Science

By

JASON DENNIS ESSELBURN
B.S., Muskingum College, 2007

2009
Wright State University

WRIGHT STATE UNIVERSITY

SCHOOL OF GRADUATE STUDIES

June 11, 2009

I HEREBY RECOMMEND THAT THE THESIS PREPARED UNDER MY SUPERVISION BY Jason D. Esselburn ENTITLED Porosity and Permeability in Ternary Sediment Mixtures BE ACCEPTED IN PARTIAL FULFILLMENT OF THE REQUIREMENTS FOR THE DEGREE OF Master of Science.

_____

Robert W. Ritzi, Ph.D.
Thesis Co-Director

_____

David F. Dominic, Ph.D.
Thesis Co-Director

_____

David F. Dominic, Ph.D.
Department Chair

Committee on
Final Examination

_____

Robert W. Ritzi, Ph.D.
Thesis Co-Director

_____

David F. Dominic, Ph.D.
Thesis Co-Director

_____

Allen Hunt, Ph.D.

_____

Joseph F. Thomas, Jr., Ph.D.
Dean, School of Graduate Studies

ABSTRACT

Esselburn, Jason D., M.S., Department of Earth and Environmental Sciences, Wright State University, 2009. Porosity and Permeability in Ternary Sediment Mixtures.

Porosity and permeability were measured in mixtures of fine, medium, and coarse sand, where the volume fraction of each of the three components was systematically varied. The porosity varies non-linearly with the volume fractions, and can be modeled with a piecewise-linear approach. The permeability also varies non-linearly with the volume fractions. Permeability can be modeled with the Kozeny-Carman equation using a recursive approach for computing the representative grain size from those of the components in the mixture.

TABLE OF CONTENTS

LIST OF FIGURES

LIST OF TABLES

ACKNOWLEDGEMENTS

I would like to express my gratitude to all those who have supported this thesis. I thank Dr. Robert Ritzi, Dr. David Dominic, and Dr. Allen Hunt for their guidance throughout the project as research advisors. Also, special thanks goes to Jim Ferreira, Larry Mastera, Arijit Guin, Ramya Ramanathan, Melissa Kennedy, Stephen Sadurski, Alyssa Grissom, and my parents Jim and Jenny for their assistance and support.

1.0 INTRODUCTION

In many applications, sediment is often represented by a single grain size (usually the mean) but all natural sediments comprise distributions of sizes. For such sediments, the porosity, ϕ, and the permeability, k, vary non-linearly with the proportion of each grain size component (Kamann, et al., 2007). Figure 1 illustrates this for bimodal mixtures of coarser and finer grains. This figure shows that as the proportion of finer grains increases from zero, ϕ and k decrease as pore spaces between coarser grains become increasingly filled with finer grains. If the finer grains are smaller than the pores among the coarser grains, they can occupy those pores without disturbing the packing (coarse packing). Otherwise, individual finer grains prevent the coarser grains from attaining the packing they would have in the absence of the finer grains (disturbed coarse packing). When the volume content of finer grains equals the ϕ of the coarser grains alone, ϕ and k are at a minimum. At still higher proportions of finer grains, coarser grains are individually supported by a matrix of finer grains (fine packing). In this case, the coarser grains act as non-porous, non-permeable "baffles." As the proportion of finer grains increases beyond this point, ϕ and k increase because the volume of such baffles decreases.

Focusing on ϕ, it is known that mixtures of uniform spheres with two grain sizes do not pack as ideal coarse packing or ideal fine packing (Koltermann and Gorelick,

1995). Though one type of packing may dominate, regions of different packing occur and the minimum ϕ is not as low as that in ideal mixtures (i.e. uniform packing).

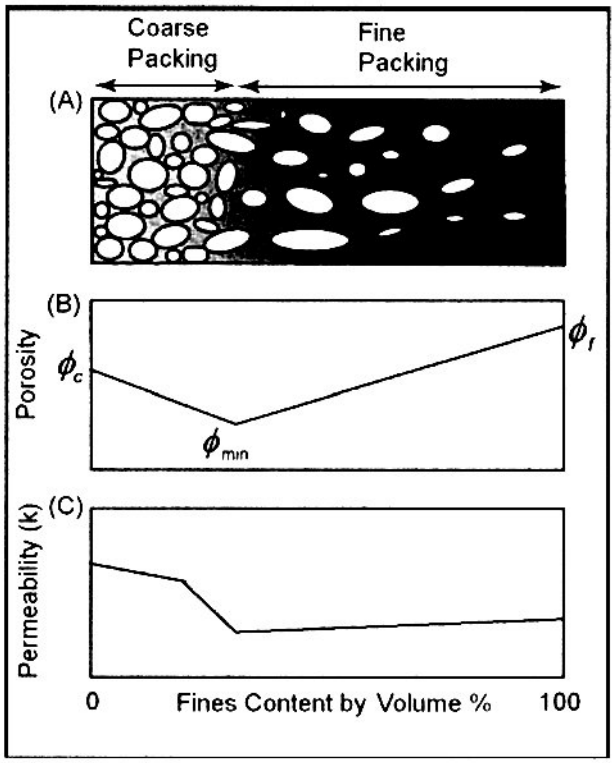

Figure 1: (A) Conceptual model of grain packing for a two-component sediment mixture. (B) Porosity within a sediment mixture with respect to the volume fraction of fines (in regions of both coarse and fine packing). The symbols ϕ_{min}, ϕ_c and ϕ_f refer to the absolute porosity minimum, porosity of the coarser component only, and the porosity of the finer component only, respectively. (C) Observed changes in permeability as a function of the volume fraction of fines. (Kamann et al., 2007, as modified from Koltermann and Gorelick, 1995).

There is no practical way to determine the relative volumes of each packing arrangement, and models for porosity cannot be derived from first principles (Koltermann and Gorelick, 1995). Models for porosity in sediment mixtures are empirical. As Figure 1B suggests, piecewise-linear interpolation works well. For a two-component model, Kamann et al. [2007] showed that the following piecewise-linear function works well:

$$\phi = \phi_c - \left[\frac{\phi_c - \phi_{min}}{\phi_c}\right]\xi_f \; ; \;\; \xi_f \leq \phi_c \qquad [1]$$

$$\phi = \phi_f + \left[\frac{\phi_f - \phi_{min}}{1 - \phi_c}\right](\xi_f - 1) \; ; \;\; \xi_f \geq \phi_c \qquad [2]$$

where ϕ_f is the porosity of the finer component only, ϕ_c is the porosity of the coarser component only, ϕ_{min} is the porosity minimum at which the volume of fines is equal to the pore volume of the coarse grains. These three values must be known. ξ_f is the premixed volume fraction of fines ($V_f/(V_f+V_c)$). ξ_f is fundamentally different from the postmixed volume fraction of fines (V_f/V_T) because, when mixed, the total sample volume (V_T) is often less than the sum of its component volumes (V_f+V_c). The postmixed volume fraction of fines will be referred to as r_f.

Figure 2 shows how porosity varies in a three-component mixture. The global porosity minimum occurs where the volume fraction of the finest component is approximately equal to the ϕ of the coarsest component (approximately 40% ‘small’ and 60% ‘large’ in the figure).

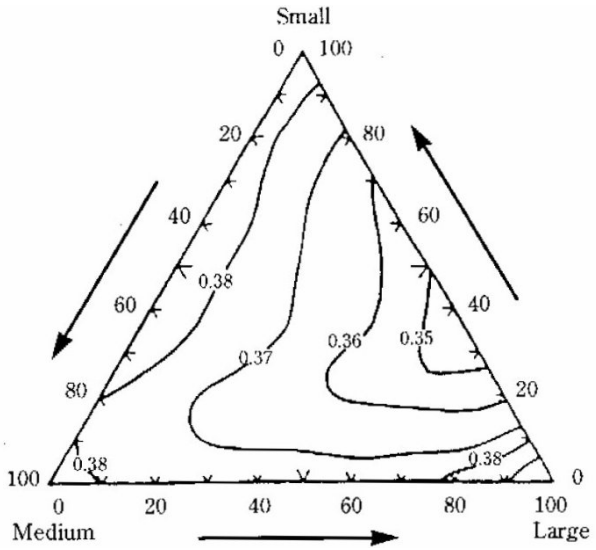

Figure 2: Porosity in a three-component mixture of spherical glass beads (Yu and Zou, 1998). On each axis is the percent volume of each component.

Again, empirical models based on piecewise-linear interpolation work well. Regression approaches that have been published (Standish and Yu, 1987; Yu and Zou, 1998) require knowing ϕ at seven points on the ternary axes: ϕ_f, ϕ_c, ϕ_m which is the porosity of the medium component, $\phi_{min(f\text{-}c)}$ which is the porosity minimum on the fine-coarse axis (the global minimum), $\phi_{min(f\text{-}m)}$ which is the porosity minimum on the fine-medium axis, $\phi_{min(m\text{-}c)}$ which is the porosity minimum on the medium-coarse axis, and $\phi_{f=m=c}$ which is the porosity of the mixture of $33.\overline{3}$ % of each component.

One goal of this study was to develop a more parsimonious piecewise-linear model than in prior approaches. The approach of this study was to use piecewise-planar models as illustrated in Figure 3. The two-plane model (Figure 3A) requires knowing four measured porosities. The four-plane model (Figure 3B) requires knowing six measured porosities. Importantly, the two-plane and the four-plane model require knowing ϕ for single and two-component mixtures. For comparison, a six-plane model

(Figure 3C) was also used which requires seven measured porosities including the ϕ for a three-component mixture ($\xi_f = \xi_m = \xi_c$) as with prior published models.

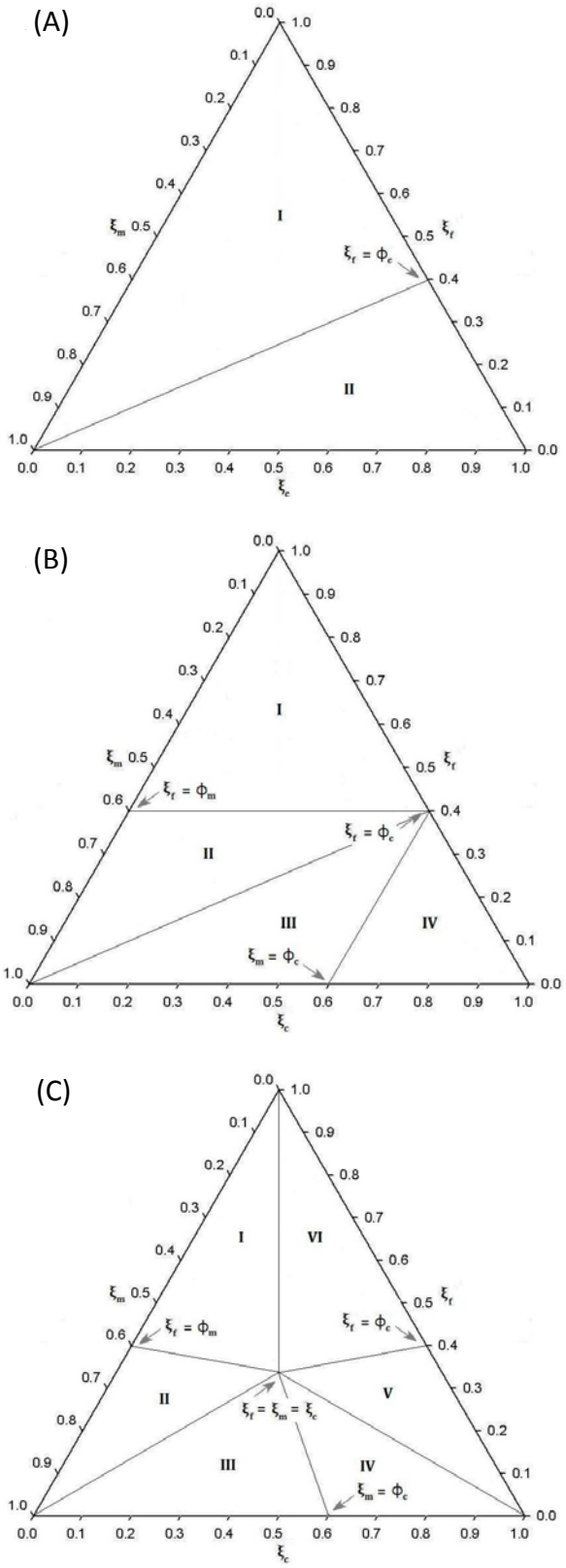

Figure 3: Annotated diagrams of each of the porosity models derived for this study: (A) two-plane, (B) four-plane, and (C) six-plane models.

The two-plane model is given by:

$$\phi = \xi_f \phi_f + \xi_m \phi_m + \xi_c \frac{\phi_{\min(f-c)} - \phi_f \phi_c}{(1-\phi_c)};\ \ Region\ I \quad [3]$$

$$\phi = \xi_f \frac{\phi_{\min(f-c)} - \phi_c(1-\phi_c)}{\phi_c} + \xi_m \phi_m + \xi_c \phi_c\ ;\ \ Region\ II \quad [4]$$

the four-plane model is given by:

$$\phi = \xi_f \phi_f + \xi_m \frac{\phi_{\min(f-m)} - \phi_f \phi_m}{1-\phi_m} + \xi_c \frac{\phi_{\min(f-c)} - \phi_f \phi_c}{1-\phi_c};\ Region\ I \quad [5]$$

$$\phi = \xi_f \frac{\phi_{\min(f-m)} - \phi_m(1-\phi_m)}{\phi_m} + \xi_m \phi_m + \xi_c \frac{\phi_{\min(f-c)} - \phi_c\left[\frac{\phi_{\min(f-m)} - \phi_m(1-\phi_m)}{\phi_m}\right]}{1-\phi_c};\ Region\ II \quad [6]$$

$$\phi = \xi_f \frac{\phi_{\min\,(f-c)} - (1-\phi_c)\left[\frac{\phi_{\min(m-c)} - \phi m \phi_c}{1-\phi_c}\right]}{\phi_c} + \xi_m \phi_m + \xi_c \frac{\phi_{\min(m-c)} - \phi_m \phi_c}{1-\phi_c};\ Region\ III \quad [7]$$

$$\phi = \xi_f \frac{\phi_{\min(f-c)} - \phi_c(1-\phi_c)}{\phi_c} + \xi_m \frac{\phi_{\min(m-c)} - \phi_c(1-\phi_c)}{\phi_c} + \xi_c \phi_c\ ;\ Region\ IV \quad [8]$$

and the six-plane model is given by:

$$\phi = \xi_f \phi_f + \xi_m \frac{\phi_{\min(f-m)} - \phi_f \phi_m}{1-\phi_m} + \xi_c \frac{\phi_{f=m=c} - 0.33\phi_f + 0.33\left[\frac{\phi_{\min\,(f-m)} - \phi_f \phi_m}{1-\phi_m}\right]}{0.33};\ \ Region\ I \quad [9]$$

$$\phi = \xi_f \frac{\phi_{\min(f-m)} - \phi_m(1-\phi_m)}{\phi_m} + \xi_m \phi_m + \xi_c \frac{\phi_{f=m=c} - 0.33\phi_m + 0.33\left[\frac{\phi_{\min(f-m)} - \phi_m(1-\phi_m)}{\phi_m}\right]}{0.33};\ Region\ II \quad [10]$$

$$\phi = \xi_f \frac{\phi_{f=m=c} - 0.33\phi_m - 0.33\left[\frac{\phi_{\min(m-c)} - \phi_m \phi_c}{1-\phi_c}\right]}{0.33} + \xi_m \phi_m + \xi_c \frac{\phi_{\min(m-c)} - \phi_m \phi_c}{1-\phi_c};\ \ Region\ III \quad [11]$$

$$\phi = \xi_f \frac{\phi_{f=m=c} - 0.33\left[\frac{\phi_{\min(m-c)} - \phi_c(1-\phi_c)}{\phi_c}\right]}{0.33} + \xi_m \frac{\phi_{\min\,(m-c)} - \phi_c(1-\phi_c)}{\phi_c} + \xi_c \phi_c\ ;\ \ Region\ IV \quad [12]$$

$$\phi = \xi_f \frac{\phi_{\min(f-c)} - \phi_c(1-\phi_c)}{\phi_c} + \xi_m \frac{\phi_{f=m=c} - 0.33\left[\frac{\phi_{\min(f-c)} - \phi_c(1-\phi_c)}{\phi_c}\right] - 0.33\phi_c}{0.33} + \xi_c \phi_c\ ;\ \ Region\ V \quad [13]$$

$$\phi = \xi_f \phi_f + \xi_m \frac{\phi_{f=m=c} - 0.33\phi_f - 0.33\left[\frac{\phi_{\min(f-c)} - \phi_f \phi_c}{1-\phi_c}\right]}{0.33} + \xi_c \frac{\phi_{\min(f-c)} - \phi_f \phi_c}{1-\phi_c};\ \ Region\ VI \quad [14]$$

The methods used to evaluate each of these models are given in the next section.

Permeability can be modeled in two-component sediment mixtures quite well by a form of the Kozeny-Carman equation:

$$k = \frac{d^2\phi^3}{180(1-\phi)^2} \quad [15]$$

where k is the estimated intrinsic permeability of the sediment mixture and d is the representative grain diameter of the sediment mixture. In two-component mixtures, the harmonic mean is used when $\xi_f \geq \phi_c$ and the geometric mean is used when $\xi_f < \phi_c$. ϕ can be a measured value, or one of the ϕ models given above (Koltermann and Gorelick, 1995; Kamann et al., 2007; Phillips, 2007; and Conrad et al., 2008).

Note that Chapuis and Aubertin [2003] have also considered using the Kozeny-Carman equation for multicomponent mixtures but use the harmonic mean for all ξ_f. (Note that Chapuis and Aubertin [2003] write the Kozeny-Carman equation with different variables, e.g. void ratio instead of porosity, but it is easy to show that their version is exactly equivalent to Equation 15). The exclusive use of the harmonic mean in their approach causes the systematic underprediction of permeability when $\xi_f < \phi_c$.

We applied a logical extension of Koltermann and Gorelick's [1995] approach to using the Kozeny-Carman equation (Equation 15) to three-component sediment mixtures. Parameter d is computed in two recursive steps based on two conditions. Condition A is $\xi_f > \phi_m$, so that the medium component's pore space is filled by fines. Condition B is $\xi_f + \xi_m > \phi_c$, so that the coarse component's pore space is filled by finer components. In step 1, if A is true, the harmonic mean, d_H, is taken of the fine and medium grain sizes, d_f and d_m. Otherwise, the geometric mean, d_G, is taken. In step 2, if B is true, d_H is taken between the coarse grain size, d_c, and the result from step 1. Otherwise, d_G is taken. In all

cases, d_H and d_G are computed as weighted by ξ_f, ξ_m, and ξ_c. This procedure is conveyed in Table 1 and Figure 4.

Table 1: Approach to computing d

	A True	**A False**
B True	Step 1: d_H for d_m and d_f Step 2: d_H for d_c and step 1 result	Step 1: d_G for d_m and d_f Step 2: d_H for d_c and step 1 result
B False	Step 1: d_H for d_m and d_f Step 2: d_G for d_c and step 1 result	Step 1: d_G for d_m and d_f Step 2: d_G for d_c and step 1 result

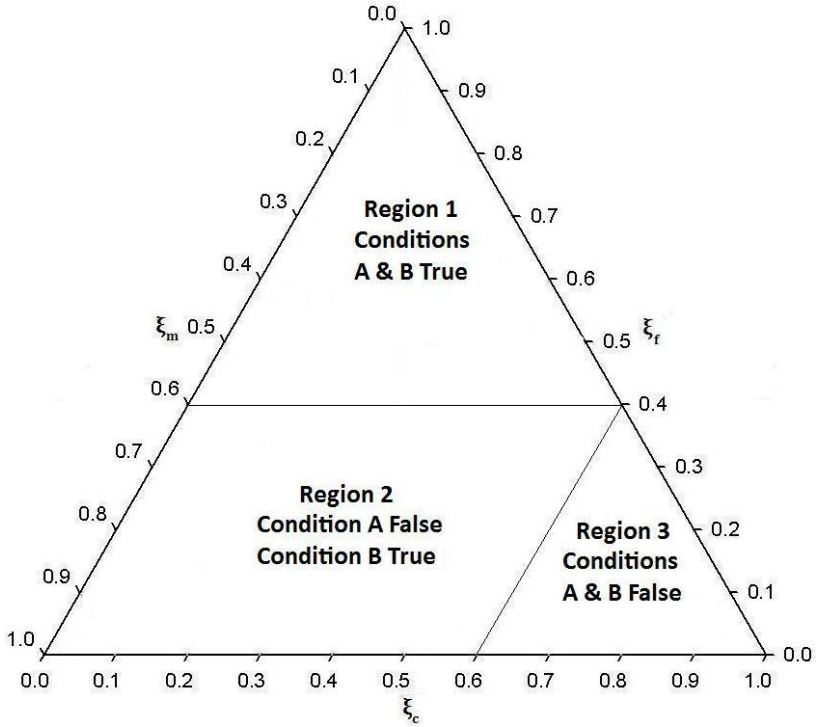

Figure 4: Regions corresponding to Table 1.

The example in Figure 4 is for a mixture of three sizes of spheres. Spheres of one size, when stirred under friction, have a porosity of 0.4 (Gray, 1968; German, 1989; Kamann et al., 2007) and thus $\phi_f = \phi_m = \phi_c$. In this case, if A is true, then B must be true so there are only three regions possible. Spheres were used as model sediment in this study as described in the next section.

In summary, the objectives of this study were to [1] expand the piecewise-linear porosity model of Kamann et al. [2007] to three-component sediment mixtures and evaluate how many piecewise-planar elements are needed, and [2] test the use of the Kozeny-Carman equation using d as given in Table 1.

2.0 METHODOLOGY

2.1 SEDIMENT MIXTURES

The methodologies used in this study are generally consistent with those of Kamann et al. [2007]. Porosity and permeability were experimentally determined for sediment mixtures in which the volume fractions of components were systematically varied. These data were then used as the basis for assessing the models. Spherical sandblasting beads were sorted into fine, medium, and coarse sand sizes, as in Table 2.

Table 2: Physical attributes of the different sediments used in this study

Sediment	Grain Diameter [mm]	Retained on Sieve #	Porosity [-]	Approximate Pore Size [mm]
Fine Sand	0.165	100	0.4	0.068
Medium Sand	0.390	45	0.4	0.159
Coarse Sand	0.655	30	0.4	0.269

The beads were sorted into the narrowest range possible with commercially available sieves. The coarse sand has a diameter that is retained between 0.590 and 0.710 mm sieve screens, the medium sand is retained between 0.350 and 0.420 mm sieve screens, and the fine sand fits between 0.148 and 0.177 mm sieve screens. Note that a fine-coarse sand mixture allows for ideal coarse packing, but that a fine-medium or medium-coarse sand mixture will cause disturbed packing (Kamann et al., 2007).

2.2 POROSITY MEASUREMENT

To measure effective porosity, a burette was used to decant water into the sediment sample. The test chamber (a beaker of appropriate size) was held in a tilted

orientation, allowing the water to displace the air in the sample pores. A premixed volume of 100 cm^3 (i.e. $V_f + V_m + V_c = 100\ cm^3$) was used for all sand-sized mixtures, and measured the postmixed volume V_T. Porosity was computed from the ratio of the volume of water required to saturate the pores per V_T.

Kamann et al. [2007] already measured porosity in two-component mixtures of these grain sizes. Five test points were selected that contain three components as given in Table 3:

Table 3: Premixed volume fractions used to create each sample

Test Point	ξ_f	ξ_m	ξ_c
1	0.666	0.166	0.166
2	0.166	0.666	0.166
3	0.166	0.166	0.666
4	0.333	0.333	0.333
5	0.133	0.433	0.433

Three measurements were made for each test point. The summary statistics for the porosity data are reported in appendix A.

2.3 PERMEABILITY MEASUREMENT

Permeability was measured with a constant-head permeameter. The hydraulic gradient, $\frac{\partial h}{\partial l}$, and volumetric discharge, Q, under steady-state flow were measured, as was water temperature. Water temperature was used to identify the fluid density, ρ, and viscosity, μ. The permeability was computed with the following form of Darcy's Law:

$$k = \left[Q \left(\frac{\rho g A}{\mu} \frac{\partial h}{\partial l} \right)^{-1} \right] \quad [16]$$

where A is the cross-sectional area of the sample and g is acceleration due to gravity. Measurements were collected three consecutive times for each of three different gradients for each of three samples. Thus, measurements were collected 27 times for each test point in Table 3.

3.0 RESULTS AND DISCUSSION

3.1 POROSITY MODEL RESULTS AND DISCUSSION

The measured ϕ are tabulated in Table 4. The right-hand column indicates which are used to define the two-, four-, and six-plane models (control points). Model ϕ are compared to the measured ϕ in Figure 5.

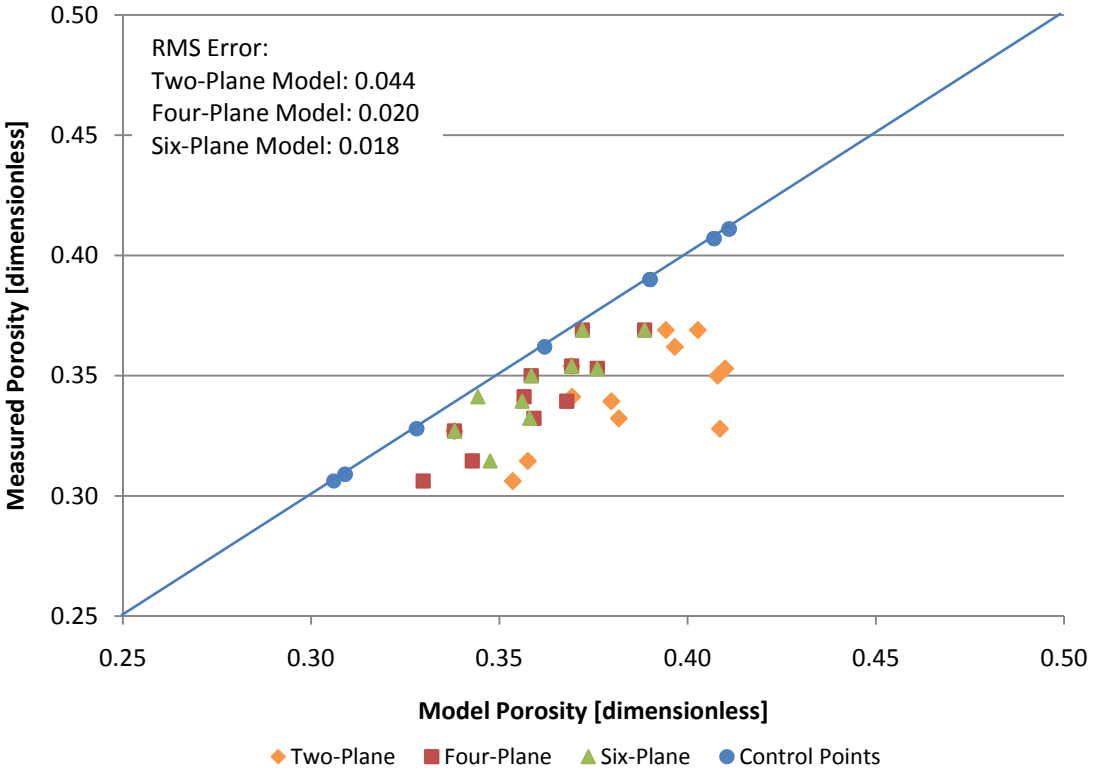

Figure 5: Comparison of the three porosity models against measured porosities. The line represents one-to-one equality in which model porosity equals measured porosity.

The models are exact linear interpolators, giving the values of the control points at those mixture percentages. None of these control points were used in evaluating the models.

All of the models have a bias that give ϕ higher than observed. The root mean of squared differences (RMS) between model and observed values was computed. The two-plane model returns RMS error of 0.044. The four-plane model returns RMS error of 0.020. The six-plane model returns a RMS error of 0.018. The four-plane model returns a RMS error that is very close to that of the six-plane model, but requires fewer measured ϕ values to interpolate from. Furthermore, it only requires ϕ be known from two-component mixtures. Therefore, it was chosen as a parsimonious model. We expect it to be useful in interpolating porosity from six control points, noting it will tend to be approximately 2% above the measured values. Its usefulness in the Kozeny-Carman model for permeability is further examined below. The four-plane model and the measured porosities of each test point are both contoured in Figure 6.

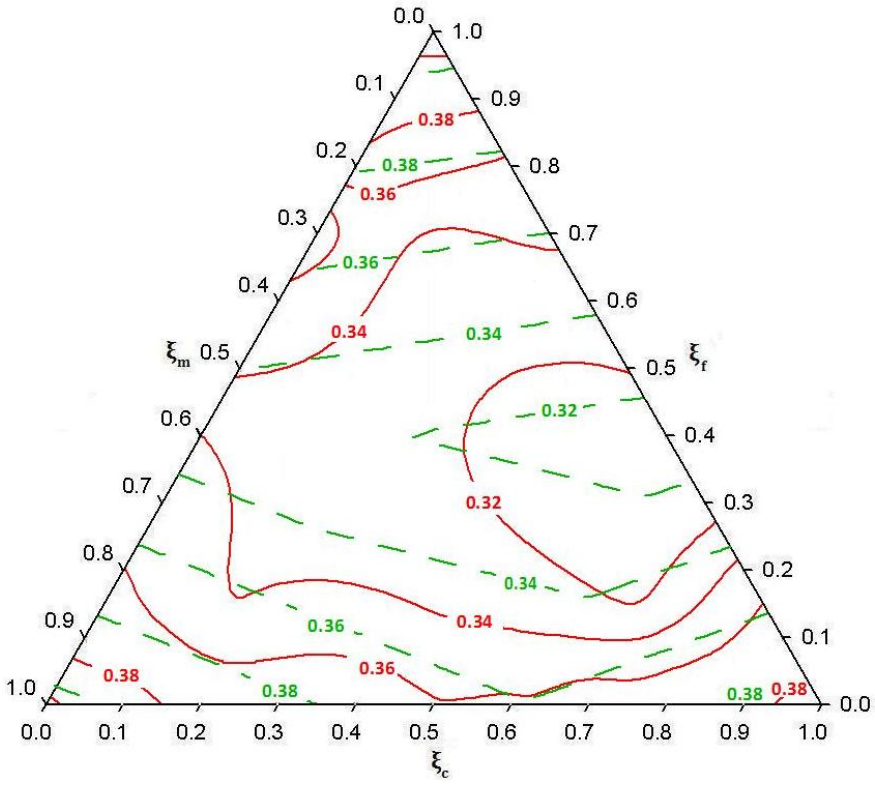

Figure 6: Contoured surface of measured porosity (red solid contours) overlain by the contoured surface of estimated porosity (green dashed contours).

Table 4: Porosity data from Kamann et al. [2007] and this study (plotted in Figure 6)

ξ_f	ξ_m	ξ_c	**Average Measured Porosity [-]**	**Model Control Point if Indicated**
0.666	0.166	0.166	0.332	--
0.166	0.666	0.166	0.339	--
0.166	0.166	0.666	0.315	--
0.333	0.333	0.333	0.306	Six-Plane
0.133	0.433	0.433	0.341	--
0.000	0.000	1.000	0.390	Two-, Four-, and Six-Plane
0.100	0.000	0.900	0.371	--
0.200	0.000	0.800	0.354	--
0.300	0.000	0.700	0.317	--
0.400	0.000	0.600	0.317	Two-, Four-, and Six-Plane
0.500	0.000	0.500	0.321	--
0.600	0.000	0.400	0.329	--
0.700	0.000	0.300	0.346	--
0.800	0.000	0.200	0.358	--
0.900	0.000	0.100	0.388	--
1.000	0.000	0.000	0.411	Two-, Four-, and Six-Plane
0.100	0.900	0.000	0.371	--
0.200	0.800	0.000	0.363	--
0.300	0.700	0.000	0.358	--
0.400	0.600	0.000	0.346	Four- and Six-Plane
0.500	0.500	0.000	0.343	--
0.600	0.400	0.000	0.358	--
0.700	0.300	0.000	0.371	--
0.800	0.200	0.000	0.379	--
0.900	0.100	0.000	0.388	--
0.000	1.000	0.000	0.407	Two-, Four-, and Six-Plane
0.000	0.100	0.900	0.378	--
0.000	0.200	0.800	0.379	--
0.000	0.300	0.700	0.377	--
0.000	0.400	0.600	0.366	Four- and Six-Plane
0.000	0.500	0.500	0.362	--
0.000	0.600	0.400	0.378	--
0.000	0.700	0.300	0.379	--
0.000	0.800	0.200	0.374	--
0.000	0.900	0.100	0.393	--

3.2 PERMEABILITY RESULTS AND DISCUSSION

The measured k values are tabulated in Table 5. The k model (Equation 15) was first computed using the measured ϕ and d following from Table 1. The computed values are compared to the measured values in Figure 7. The RMS error is 24.68. The recursive method of computing d as per Table 1, seems to give a very good result in all three regions.

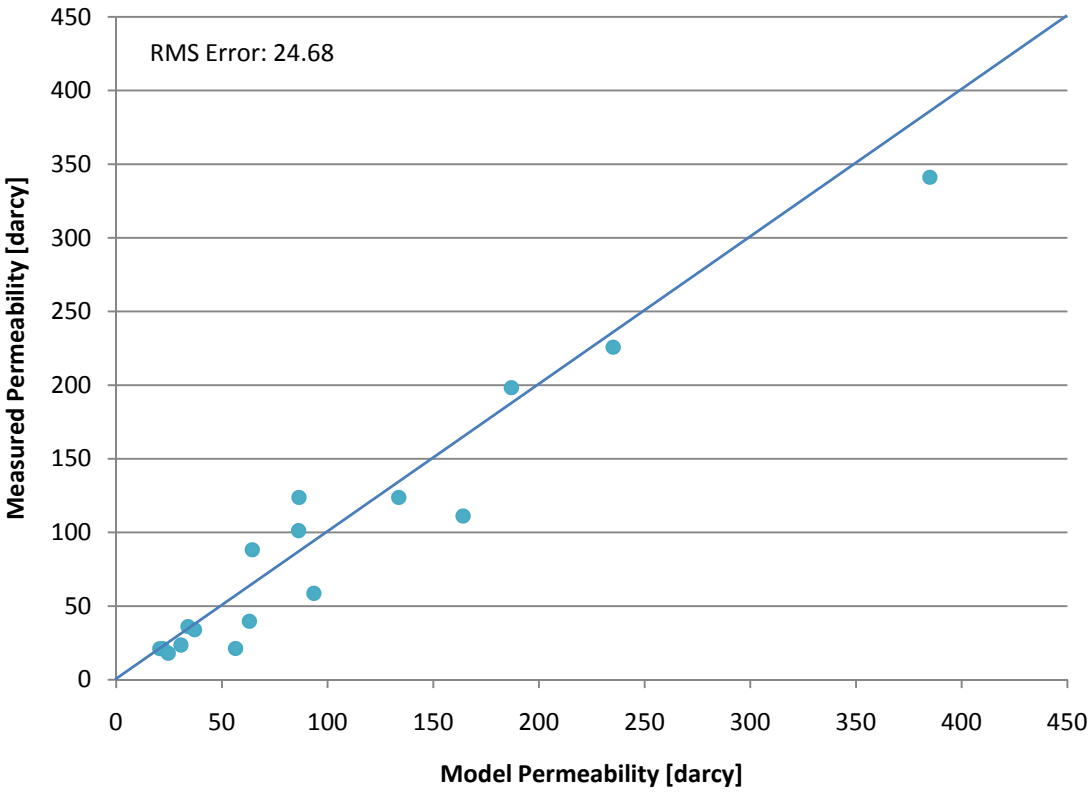

Figure 7: Comparison of the Kozeny-Carman model against measured permeabilities. The Kozeny-Carman model is here computed with measured ϕ.

Table 5: Permeability data from Conrad et al. [2008] and this study (plotted in Figures 7 and 8)

ξ_f	ξ_m	ξ_c	**Average Measured Permeability [darcy]**
0.666	0.166	0.166	20.97
0.166	0.666	0.166	86.86
0.166	0.166	0.666	123.36
0.333	0.333	0.333	35.97
0.133	0.433	0.433	101.16
1.000	0.000	0.000	23.53
0.000	1.000	0.000	111.11
0.000	0.000	1.000	341.03
0.750	0.250	0.000	21.20
0.350	0.650	0.000	33.92
0.250	0.750	0.000	21.20
0.000	0.750	0.250	123.72
0.000	0.350	0.650	198.21
0.000	0.250	0.750	225.72
0.250	0.000	0.750	58.64
0.350	0.000	0.650	39.68
0.750	0.000	0.250	17.97

The *k* model was then computed using the different ϕ models, and in each case again using the recursive method of computing *d*. The results using the two-plane ϕ model are given in Figure 8A. The results using the four-plane ϕ model are given in Figure 8B. The results using the six-plane ϕ model are given in Figure 8C.

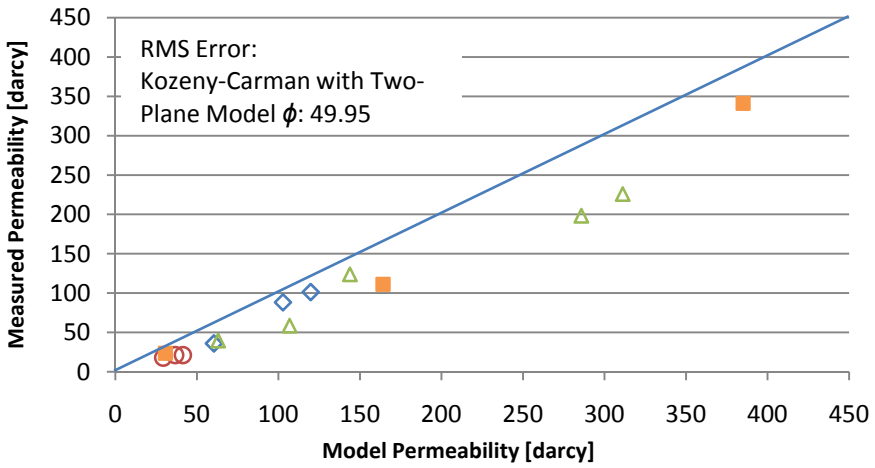

(A)

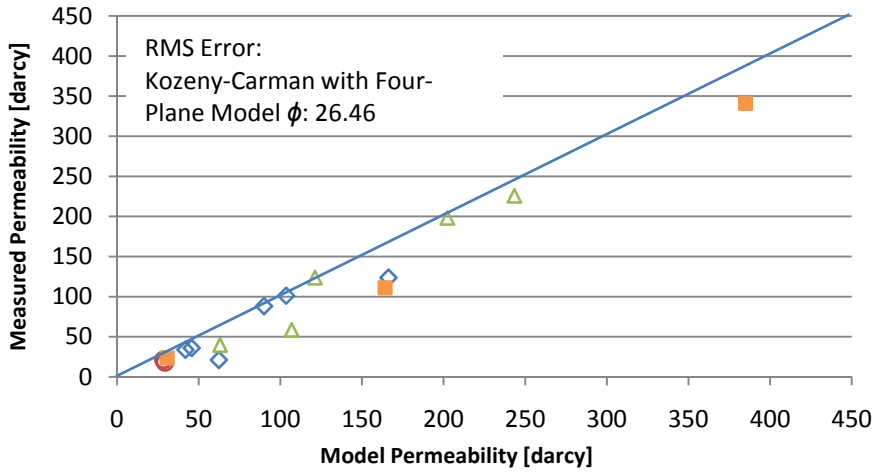

(B)

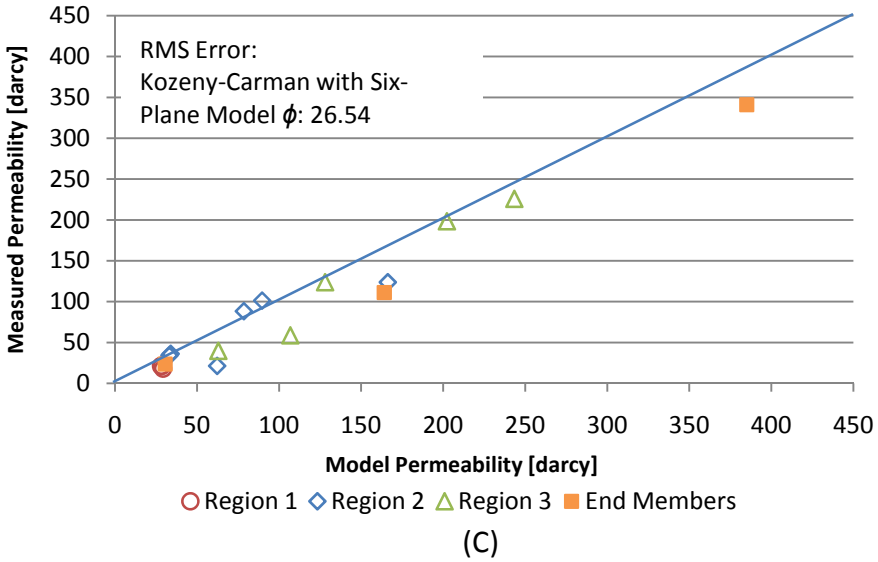

(C)

Figure 8: Comparison of the Kozeny-Carman model with (A) two-plane, (B) four-plane, and (C) six-plane ϕ models.

The RMS differences between the Kozeny-Carman model computed with the measured ϕ and the measured k are 49.95, 26.46, and 26.54 respectively (as reported in Figure 8). The RMS error between the Kozeny-Carman model computed with measured ϕ and the Kozeny-Carman computed with the model ϕ are 43.51 for the two-plane, 15.36 for the four-plane, and 14.65 for the six-plane. Appreciable improvement is observed with the use of a four-plane ϕ model versus a two-plane ϕ model in the Kozeny-Carman, and in this scenario, absolute RMS error increases with the use of a six-plane ϕ model.

To ascertain which parameter the Kozeny-Carman model is more sensitive to (d or ϕ), the partial derivative of k with respect to d and ϕ were taken and evaluated for every mixture for which permeability was measured.

$$\frac{\partial k}{\partial d} = \frac{2d\,\phi^3}{180(1-\phi)^2} \qquad [17]$$

$$\frac{\partial k}{\partial \phi} = \frac{2d}{180}\left[\frac{3\phi^2 - \phi^3}{(1-\phi)^3}\right] \qquad [18]$$

The results of this sensitivity analysis appear in Table 6.

Table 6: Sensitivity coefficients for a sampling of sediment mixtures.

ξ_f	ξ_m	ξ_c	**Sensitivity (d)**	**Sensitivity (ϕ)**
0.666	0.166	0.166	1.93E-07	2.32E-06
0.166	0.666	0.166	3.55E-07	4.21E-06
0.166	0.166	0.666	3.56E-07	4.42E-06
0.333	0.333	0.333	2.11E-07	2.67E-06
0.133	0.433	0.433	4.99E-07	5.75E-06
1.000	0.000	0.000	3.67E-07	3.92E-06
0.000	1.000	0.000	8.31E-07	8.93E-06
0.000	0.000	1.000	1.16E-06	1.27E-05
0.750	0.250	0.000	2.92E-07	3.27E-06
0.350	0.650	0.000	2.86E-07	3.40E-06
0.250	0.750	0.000	3.91E-07	4.49E-06
0.000	0.750	0.250	6.08E-07	6.87E-06
0.000	0.350	0.650	6.76E-07	7.77E-06
0.000	0.250	0.750	8.07E-07	9.12E-06
0.250	0.000	0.750	3.98E-07	4.83E-06
0.350	0.000	0.650	3.07E-07	3.80E-06
0.750	0.000	0.250	2.85E-07	3.22E-06

The results show that the Kozeny-Carman model is about ten times more sensitive to ϕ than d.

4.0 CONCLUSIONS

The results of this study show:

1) k is modeled well by the Kozeny-Carman equation for three-component mixtures if d is computed recursively. In this approach, first the d of the finer and medium grain size component are averaged using d_G if $\xi_f < \phi_m$ and d_H if $\xi_f > \phi_m$. This result is then averaged with the d of the coarser grain size component, using d_G if $\xi_f + \xi_m < \phi_c$ and d_H if $\xi_f + \xi_m > \phi_c$.

2) ϕ can be modeled well for three-component mixtures by piecewise-linear interpolation using a four-plane model. This requires less information than published approaches, and only requires knowing ϕ of the end members and ϕ_{min} for the two-component mixture combinations. All linear models over-represent ϕ. The four-plane model does so with a RMS error of about 2%.

3) k is modeled well by using the Kozeny-Carman equation with the four-plane ϕ model.

4) The Kozeny-Carman model is about ten times more sensitive to ϕ than to d in three-component mixtures of sand-sized particles.

APPENDIX A: Porosity Data and Statistics

Table A1: Porosity data for each sediment mixture

	Run #	ξ_f	ξ_m	ξ_c	Porosity [-]
Test Point 1	1	0.666	0.166	0.166	0.3323
	2	0.666	0.166	0.166	0.3301
	3	0.666	0.166	0.166	0.3344

Summary Statistics	
Mean	0.3323
Minimum	0.3301
Maximum	0.3344

	Run #	ξ_f	ξ_m	ξ_c	Porosity [-]
Test Point 2	1	0.166	0.666	0.166	0.3415
	2	0.166	0.666	0.166	0.3404
	3	0.166	0.666	0.166	0.3362

Summary Statistics	
Mean	0.3394
Minimum	0.3362
Maximum	0.3415

	Run #	ξ_f	ξ_m	ξ_c	Porosity [-]
Test Point 3	1	0.166	0.166	0.666	0.3121
	2	0.166	0.166	0.666	0.3141
	3	0.166	0.166	0.666	0.3174

Summary Statistics	
Mean	0.3145
Minimum	0.3121
Maximum	0.3174

	Run #	ξ_f	ξ_m	ξ_c	Porosity [-]
Test Point 4	1	0.333	0.333	0.333	0.3054
	2	0.333	0.333	0.333	0.3077
	3	0.333	0.333	0.333	0.3055

Summary Statistics	
Mean	0.3062
Minimum	0.3054
Maximum	0.3077

	Run #	ξ_f	ξ_m	ξ_c	Porosity [-]
Test Point 5	1	0.133	0.433	0.433	0.3358
	2	0.133	0.433	0.433	0.3427
	3	0.133	0.433	0.433	0.3452

Summary Statistics	
Mean	0.3412
Minimum	0.3358
Maximum	0.3452

APPENDIX B: Permeability Data and Statistics

Table B1: Permeability data for test point 1

	Run #	ξ_f	ξ_m	ξ_c	Measured Hydraulic Conductivity (K) [m/sec]	Measured Permeability (k) [darcy]
Test Point 1	1.1	0.666	0.166	0.166	2.20E-04	21.56
	1.2	0.666	0.166	0.166	2.09E-04	20.47
	1.3	0.666	0.166	0.166	2.14E-04	20.96
	1.4	0.666	0.166	0.166	2.13E-04	20.83
	1.5	0.666	0.166	0.166	2.15E-04	21.00
	1.6	0.666	0.166	0.166	2.21E-04	21.66
	1.7	0.666	0.166	0.166	2.17E-04	21.21
	1.8	0.666	0.166	0.166	2.16E-04	21.10
	1.9	0.666	0.166	0.166	2.18E-04	21.30
	2.1	0.666	0.166	0.166	2.20E-04	21.51
	2.2	0.666	0.166	0.166	2.09E-04	20.47
	2.3	0.666	0.166	0.166	2.14E-04	20.96
	2.4	0.666	0.166	0.166	2.13E-04	20.83
	2.5	0.666	0.166	0.166	2.15E-04	21.00
	2.6	0.666	0.166	0.166	2.21E-04	21.66
	2.7	0.666	0.166	0.166	2.17E-04	21.21
	2.8	0.666	0.166	0.166	2.16E-04	21.10
	2.9	0.666	0.166	0.166	2.18E-04	21.30
	3.1	0.666	0.166	0.166	2.18E-04	21.30
	3.2	0.666	0.166	0.166	2.07E-04	20.23
	3.3	0.666	0.166	0.166	2.12E-04	20.72
	3.4	0.666	0.166	0.166	2.08E-04	20.38
	3.5	0.666	0.166	0.166	2.10E-04	20.53
	3.6	0.666	0.166	0.166	2.16E-04	21.16
	3.7	0.666	0.166	0.166	2.11E-04	20.57
	3.8	0.666	0.166	0.166	2.10E-04	20.46
	3.9	0.666	0.166	0.166	2.12E-04	20.65
					Mean Permeability ($\bar{\omega}$):	**20.97**

Summary Statistics		
Packing 1	Mean	21.12
	Minimum	20.47
	Maximum	21.66
Packing 2	Mean	21.11
	Minimum	20.47
	Maximum	21.66
Packing 3	Mean	20.66
	Minimum	20.23
	Maximum	21.30

Table B2: Permeability data for test point 2

	Run #	ξ_f	ξ_m	ξ_c	Measured Hydraulic Conductivity (K) [m/sec]	Measured Permeability (k) [darcy]
Test Point 2	1.1	0.166	0.666	0.166	8.67E-04	85.60
	1.2	0.166	0.666	0.166	8.41E-04	83.04
	1.3	0.166	0.666	0.166	8.62E-04	85.09
	1.4	0.166	0.666	0.166	8.69E-04	85.58
	1.5	0.166	0.666	0.166	9.79E-04	96.39
	1.6	0.166	0.666	0.166	9.52E-04	93.76
	1.7	0.166	0.666	0.166	8.67E-04	85.60
	1.8	0.166	0.666	0.166	8.41E-04	83.04
	1.9	0.166	0.666	0.166	8.62E-04	85.09
	2.1	0.166	0.666	0.166	8.69E-04	85.58
	2.2	0.166	0.666	0.166	9.79E-04	96.39
	2.3	0.166	0.666	0.166	9.52E-04	93.76
	2.4	0.166	0.666	0.166	8.67E-04	85.60
	2.5	0.166	0.666	0.166	8.09E-04	79.85
	2.6	0.166	0.666	0.166	8.62E-04	85.09
	2.7	0.166	0.666	0.166	4.07E-04	40.12
	2.8	0.166	0.666	0.166	9.79E-04	96.39
	2.9	0.166	0.666	0.166	9.52E-04	93.76
	3.1	0.166	0.666	0.166	8.67E-04	85.60
	3.2	0.166	0.666	0.166	8.41E-04	83.04
	3.3	0.166	0.666	0.166	8.62E-04	85.09
	3.4	0.166	0.666	0.166	8.69E-04	85.58
	3.5	0.166	0.666	0.166	9.79E-04	96.39
	3.6	0.166	0.666	0.166	9.52E-04	93.97
	3.7	0.166	0.666	0.166	8.69E-04	85.58
	3.8	0.166	0.666	0.166	9.79E-04	96.39
	3.9	0.166	0.666	0.166	9.52E-04	93.76
					Mean Permeability ($\bar{\omega}$):	**86.86**

Summary Statistics		
Packing 1	Mean	87.02
	Minimum	83.04
	Maximum	96.39
Packing 2	Mean	84.06
	Minimum	40.12
	Maximum	96.39
Packing 3	Mean	89.49
	Minimum	83.04
	Maximum	96.39

Table B3: Permeability data for test point 3

	Run #	ξ_f	ξ_m	ξ_c	Measured Hydraulic Conductivity (K) [m/sec]	Measured Permeability (k) [darcy]
Test Point 3	1.1	0.166	0.166	0.666	1.34E-03	132.93
	1.2	0.166	0.166	0.666	1.29E-03	127.64
	1.3	0.166	0.166	0.666	1.37E-03	135.32
	1.4	0.166	0.166	0.666	1.24E-03	123.68
	1.5	0.166	0.166	0.666	1.21E-03	120.44
	1.6	0.166	0.166	0.666	1.21E-03	120.50
	1.7	0.166	0.166	0.666	1.22E-03	121.32
	1.8	0.166	0.166	0.666	1.23E-03	122.80
	1.9	0.166	0.166	0.666	1.23E-03	122.17
	2.1	0.166	0.166	0.666	1.23E-03	121.55
	2.2	0.166	0.166	0.666	1.20E-03	118.51
	2.3	0.166	0.166	0.666	1.19E-03	118.14
	2.4	0.166	0.166	0.666	1.34E-03	133.06
	2.5	0.166	0.166	0.666	1.29E-03	127.76
	2.6	0.166	0.166	0.666	1.37E-03	135.45
	2.7	0.166	0.166	0.666	1.24E-03	123.80
	2.8	0.166	0.166	0.666	1.21E-03	120.56
	2.9	0.166	0.166	0.666	1.21E-03	120.61
	3.1	0.166	0.166	0.666	1.22E-03	121.43
	3.2	0.166	0.166	0.666	1.23E-03	122.92
	3.3	0.166	0.166	0.666	1.23E-03	122.29
	3.4	0.166	0.166	0.666	1.23E-03	121.67
	3.5	0.166	0.166	0.666	1.20E-03	118.62
	3.6	0.166	0.166	0.666	1.19E-03	118.25
	3.7	0.166	0.166	0.666	1.23E-03	122.09
	3.8	0.166	0.166	0.666	1.20E-03	118.74
	3.9	0.166	0.166	0.666	1.19E-03	118.36
					Mean Permeability ($\bar{\omega}$):	**123.36**

Summary Statistics		
Packing 1	Mean	125.20
	Minimum	120.44
	Maximum	135.32
Packing 2	Mean	124.38
	Minimum	118.14
	Maximum	135.45
Packing 3	Mean	120.49
	Minimum	118.25
	Maximum	122.92

Table B4: Permeability data for test point 4

	Run #	ξ_f	ξ_m	ξ_c	Measured Hydraulic Conductivity (K) [m/sec]	Measured Permeability (k) [darcy]
Test Point 4	1.1	0.333	0.333	0.333	3.73E-04	36.70
	1.2	0.333	0.333	0.333	3.72E-04	36.82
	1.3	0.333	0.333	0.333	3.70E-04	36.77
	1.4	0.333	0.333	0.333	3.71E-04	37.11
	1.5	0.333	0.333	0.333	3.65E-04	36.49
	1.6	0.333	0.333	0.333	3.60E-04	35.96
	1.7	0.333	0.333	0.333	3.55E-04	35.16
	1.8	0.333	0.333	0.333	3.55E-04	35.13
	1.9	0.333	0.333	0.333	3.48E-04	34.43
	2.1	0.333	0.333	0.333	3.75E-04	36.98
	2.2	0.333	0.333	0.333	3.69E-04	36.53
	2.3	0.333	0.333	0.333	3.73E-04	37.06
	2.4	0.333	0.333	0.333	3.69E-04	36.89
	2.5	0.333	0.333	0.333	3.67E-04	36.71
	2.6	0.333	0.333	0.333	3.58E-04	35.75
	2.7	0.333	0.333	0.333	3.59E-04	35.48
	2.8	0.333	0.333	0.333	3.52E-04	34.82
	2.9	0.333	0.333	0.333	3.45E-04	34.12
	3.1	0.333	0.333	0.333	3.67E-04	36.15
	3.2	0.333	0.333	0.333	3.75E-04	37.11
	3.3	0.333	0.333	0.333	3.64E-04	36.20
	3.4	0.333	0.333	0.333	3.74E-04	37.34
	3.5	0.333	0.333	0.333	3.61E-04	36.05
	3.6	0.333	0.333	0.333	3.62E-04	36.18
	3.7	0.333	0.333	0.333	3.49E-04	34.55
	3.8	0.333	0.333	0.333	3.58E-04	35.46
	3.9	0.333	0.333	0.333	3.36E-04	33.23
					Mean Permeability ($\bar{\omega}$):	**35.97**

Summary Statistics		
Packing 1	Mean	36.07
	Minimum	34.43
	Maximum	37.11
Packing 2	Mean	36.04
	Minimum	34.12
	Maximum	37.06
Packing 3	Mean	35.81
	Minimum	33.23
	Maximum	37.34

Table B5: Permeability data for test point 5

	Run #	ξ_f	ξ_m	ξ_c	Measured Hydraulic Conductivity (K) [m/sec]	Measured Permeability (k) [darcy]
Test Point 5	1.1	0.133	0.433	0.433	8.43E-04	103.12
	1.2	0.133	0.433	0.433	8.17E-04	100.03
	1.3	0.133	0.433	0.433	8.30E-04	101.83
	1.4	0.133	0.433	0.433	8.54E-04	105.03
	1.5	0.133	0.433	0.433	8.22E-04	100.83
	1.6	0.133	0.433	0.433	8.10E-04	99.96
	1.7	0.133	0.433	0.433	8.31E-04	101.42
	1.8	0.133	0.433	0.433	8.09E-04	99.85
	1.9	0.133	0.433	0.433	7.99E-04	98.88
	2.1	0.133	0.433	0.433	7.85E-04	96.09
	2.2	0.133	0.433	0.433	8.38E-04	102.53
	2.3	0.133	0.433	0.433	7.72E-04	94.73
	2.4	0.133	0.433	0.433	8.76E-04	107.79
	2.5	0.133	0.433	0.433	7.63E-04	93.62
	2.6	0.133	0.433	0.433	8.32E-04	102.59
	2.7	0.133	0.433	0.433	7.72E-04	94.18
	2.8	0.133	0.433	0.433	8.31E-04	102.48
	2.9	0.133	0.433	0.433	7.42E-04	91.81
	3.1	0.133	0.433	0.433	8.64E-04	105.69
	3.2	0.133	0.433	0.433	8.38E-04	102.53
	3.3	0.133	0.433	0.433	8.51E-04	104.44
	3.4	0.133	0.433	0.433	8.76E-04	107.79
	3.5	0.133	0.433	0.433	8.43E-04	103.48
	3.6	0.133	0.433	0.433	8.32E-04	102.59
	3.7	0.133	0.433	0.433	8.53E-04	104.09
	3.8	0.133	0.433	0.433	8.31E-04	102.48
	3.9	0.133	0.433	0.433	8.21E-04	101.48
					Mean Permeability ($\bar{\omega}$):	**101.16**

Summary Statistics		
Packing 1	Mean	101.21
	Minimum	98.88
	Maximum	105.03
Packing 2	Mean	98.42
	Minimum	91.81
	Maximum	107.79
Packing 3	Mean	103.84
	Minimum	101.48
	Maximum	107.79

APPENDIX C: Detailed Sieving and Mixing Procedures

Sieving is done with a small sample size (200 cm^3 or less) to prevent "blinding" the sieve (the term applied to when material occludes the sieve's screen and compromises throughput performance). A rubber stopper is used as an agitator to break up aggregates of glass beads, which change pore geometry. Quality control is exerted by visual inspection of the sediment with a binocular microscope. Aggregates of the glass beads and fractured glass beads are removed as detected to maintain consistent sediment shape and size.

Once the material is sieved and separated, the desired mixtures can be created by first measuring the appropriate premixed volume fractions of each component (ξ_f, ξ_m, and ξ_c), combining the mixture's constituents in a grounded mixing bowl (to prevent the accumulation of electrostatic charge which results in the formation of grain aggregates), then stirring for approximately two minutes with a wooden spoon as per Conrad [2006]. This material is then transferred to a graduated cylinder with 1 mL graduations, packed with a rod measuring 0.05 cm in diameter (to facilitate volume reduction), and V_T is measured. Once this quantity is known, the mixture can be transferred to the appropriate test chamber and the experiment run. In porosity experiments using sand-sized media only, a premixed sample volume of 100 cm^3 is used. In porosity experiments in which there are pebble-sized sediments, 400 cm^3 is the appropriate sample size (Conrad, 2006).

APPENDIX D: Detailed Porosity Procedures

Similar to the methods of Kamann et al. [2007] and Phillips [2007], a water saturation method was used to measure effective porosity. The significant difference, however, is that my method uses a burette to decant water into the test mixture. The burette's finer graduations (0.1 mL) add more certainty to the porosity measurements. The apparatus used appears in Figure D1. Conrad [2006] asserted that a representative elementary volume of 100 cm^3 (premixed) of sediment should be used for the porosity measurements when the mixture's components are all sand-sized while 400 cm^3 (premixed) should be tested when it is a sand/gravel mixture. Subscribing to this practice, I used a premixed volume of 100 cm^3 (i.e. $V_f + V_m + V_c = 100\ cm^3$) for all sand-sized mixtures.

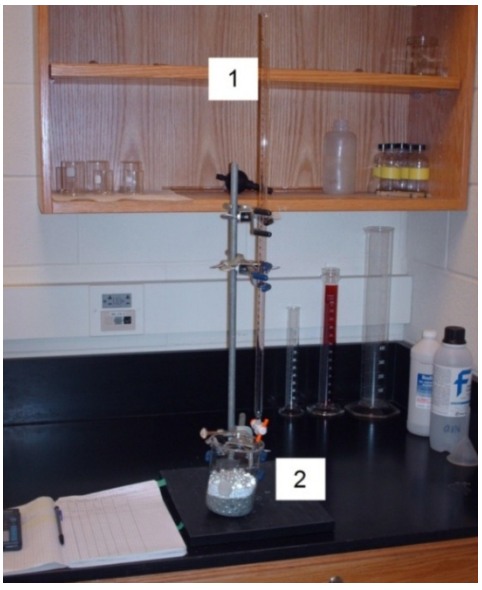

Figure D1: The setup used to measure effective porosity (ϕ) in the laboratory. This apparatus includes [1] a burette to decant water into the test chamber, and [2] a three-component sediment mixture in the test chamber.

APPENDIX E: Detailed Permeametry Procedures

Constant head permeametry has been shown to produce repeatable, accurate permeability data when used by Kamann et al. [2007], Phillips [2007], and Conrad et al. [2008]. Using Darcy's Law, the intrinsic permeability (k) can be computed. Figure E1 shows all components of the constant head permeameter apparatus.

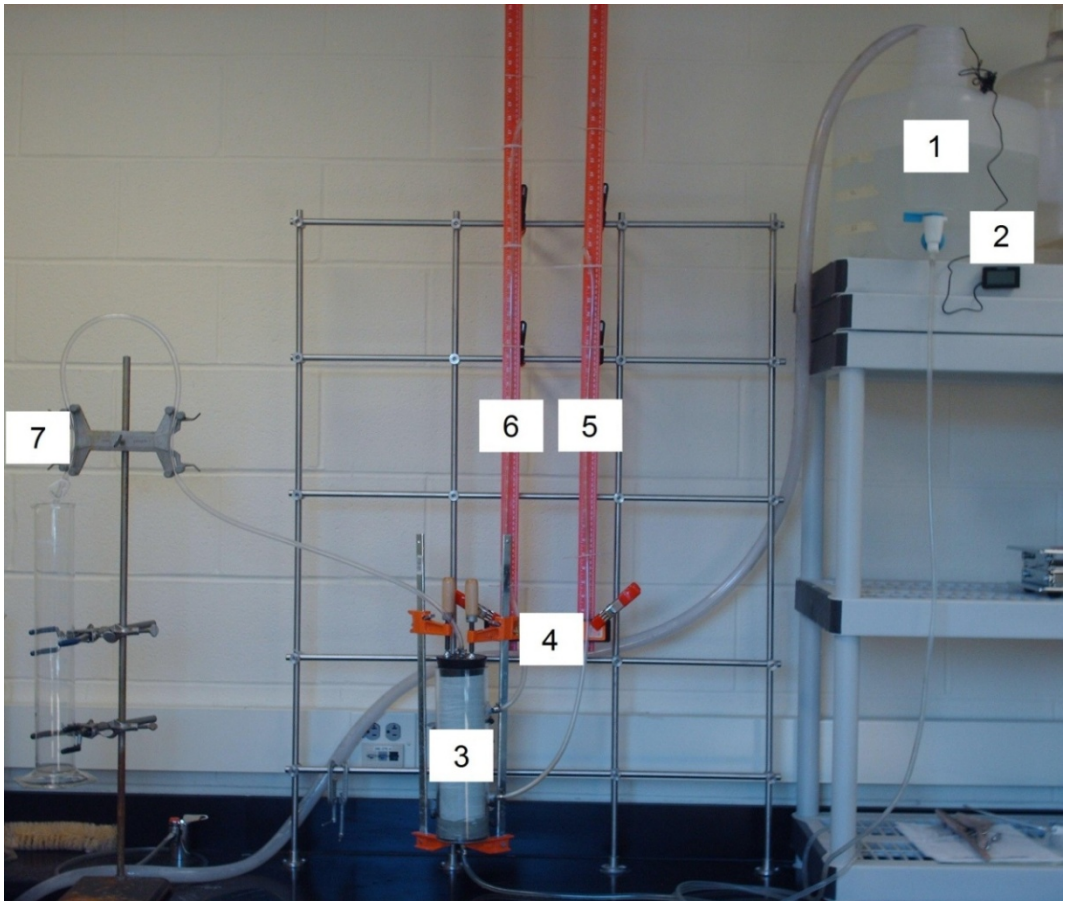

Figure E1: The setup used to measure hydraulic conductivity (K) and intrinsic permeability (k) in the laboratory. [1] is the constant head carboy, [2] is a digital thermometer (hydraulic properties of water are temperature-dependent), [3] is a three-component mixture in the permeameter tube, [4] is the elevation datum for head measurements, [5] is manometer tube 1, [6] is manometer tube 2, and [7] is the graduated cylinder where discharged water is collected and measured.

Each constant head measurement is done three consecutive times under three different gradients (done by adjusting the pressure component of head in the upgradient carboy). The permeameter tube is emptied, and then repacked with sediment that has been mixed in the appropriate volume fractions. This is done three times for a total of 27 measurements (three measurements at discharges of 100 mL, 200 mL, and 300 mL under three gradient conditions for three packings).

REFERENCES

Barr, D.W. 2001. Coefficient of permeability determined by measurable parameters. *Ground Water* 39, no. 3: 356-361.

Carman, P.C. 1937. Fluid flow through granular beds. *Transactions of the Institution of Chemical Engineers* 15: 4-20.

Chapuis, R.P. 2004. Predicting the saturated hydraulic conductivity of sand and gravel using effective diameter and void ratio. *Canadian Geotechnical Journal* 41, no. 5: 787-795.

Chapuis, R.P. and M. Aubertin. 2003. On the use of the Kozeny-Carman equation to predict the hydraulic conductivity of soils. *Canadian Geotechnical Journal* 40, no. 3: 616-628.

Clarke, R.H. 1979. Reservoir properties of conglomerates and conglomeratic sandstones. *AAPG Bulletin* 63, no. 5: 799-809.

Conrad, C.M. 2006. Air-based measurements of permeability in pebbly sands. Masters thesis, Department of Geological Sciences, Wright State University, Dayton, OH.

Conrad, C.M., R.W. Ritzi, and D.F. Dominic. 2008. Air-based measurements of permeability in pebbly sands. *Ground Water* 46, no. 1: 103-112.

Freeze, R.A. and J.A. Cherry. 1979. *Groundwater*. Prentice-Hall International, Englewood Cliffs, N.J.

German, R.M. 1989. *Particle Packing Characteristics*. Metal Powder Industries Federation, Princeton, N.J.

Gray, W.A. 1968. *The Packing of Solid Particles*. Chapman and Hall, London.

Hubbert, M.K. 1940. The theory of groundwater motion. *Journal of Geology* 48: 795-944.

Kamann, P.J. 2004. Porosity and permeability in sediment mixtures. Masters thesis, Department of Geological Sciences, Wright State University, Dayton, OH.

Kamann, P.J., R.W. Ritzi, D.F. Dominic, and C.M. Conrad. 2007. Porosity and permeability in sediment mixtures. *Ground Water* 45, no. 4: 429-438.

Koltermann, C.E. and S.M. Gorelick. 1995. Fractional packing model for hydraulic conductivity derived from sediment mixtures. *Water Resources Research* 31, no. 12: 3283-3297.

Kozeny, J. 1927. Uber kapillare leitung des wassers in Boden, Sitzungsber. *Akademie der Mathematisch-Naturwissenschaftliche Klasse* 136, no. 2a: 271-306.

Leitzelement, M., C.S. Lo, and J. Dodds. 1985. Porosity and permeability of ternary mixtures of particles. *Powder Technology* 41: 159-164.

Phillips, P.M. 2007. Porosity and permeability of bimodal sediment mixtures using natural sediment. Masters thesis, Department of Geological Sciences, Wright State University, Dayton, OH.

Standish, N. and A.B. Yu. 1987. Porosity calculations of ternary mixtures of particles. *Powder Technology* 49: 249-253.

Standish, N. and D.N. Collins, 1983. The permeability of ternary particulate mixtures for laminar flow. *Powder Technology* 36: 55-60.

Yu, A.B. and R.P. Zou. 1998. Prediction of the porosity of particle mixtures. *KONA Powder and Particle* 16: 68-81.

Yu, A.B., N. Standish, and A. McLean. 1993. Porosity calculation of binary mixtures of nonspherical particles. *Journal of American Ceramic Society* 76, no. 11: 2813-2816.